Thin Solid Films 548 (2013) 230–234

Contents lists available at ScienceDirect

Thin Solid Films

journal homepage: www.elsevier.com/locate/tsf

Thermal expansion of a lead sulfide nanofilm

S.I. Sadovnikov [a], N.S. Kozhevnikova [a,b,*], A.A. Rempel [a,b], A. Magerl [c]

[a] Institute of Solid State Chemistry, The Ural Branch of the Russian Academy of Sciences, Pervomaiskaya 91, Ekaterinburg 620990, Russia
[b] Ural Federal University, Mira 19, Ekaterinburg 620002, Russia
[c] Kristallographie und Strukturphysik, Universität Erlangen-Nürnberg, Staudtstr.3, Erlangen 91058, Germany

ARTICLE INFO

Article history:
Received 25 January 2013
Received in revised form 24 September 2013
Accepted 25 September 2013
Available online 7 October 2013

Keywords:
Lead sulfide
Thin films
Thermal expansion
X-ray diffraction

ABSTRACT

The thermal expansion of a lead sulfide nanofilm produced by chemical bath deposition was determined by X-ray diffraction (XRD). The thickness of the synthesized film was about 100 nm, and the average size of the coherent scattering regions as determined from XRD was about 40 nm. The lattice constant of the PbS nanofilm was measured as a function of the annealing temperature from 293 to 473 K and as a function of the annealing time at a constant temperature of 423 K. The thermal expansion coefficient derived was found almost twice as large as that for coarse-grained PbS.

1. Introduction

Owing to a narrow band gap of 0.41 eV and a high photosensitivity in the infrared range lead sulfide (PbS) found applications in optoelectronics, power engineering, and sensor based systems [1,2]. The optical and electronic properties of the PbS change when the crystallite sizes decrease below ~20–40 nm [3–5]. Thus, nanosized PbS in optical devices may expand their operation range from the infrared to the visible spectral range [6,7]. Change of lattice properties of PbS, including a thermal expansion coefficient factor, can occur at a greater size of nanoparticles owing to change of phonon spectrum and its edges.

Under normal conditions, PbS is a semiconductor with a cubic *B*1 structure [8,9]. Recent studies have shown that the crystal structure of the PbS nanofilms (thin nanostructured films) may be different. The term "nanofilm" or "nanostructured film" means that in the film the average size of the coherent scattering regions is less than 100 nm. A cubic (space group $F\bar{4}3m$) *B*3 structure was found in [10] for nonstoichiometric lead sulfide $PbS_{0.90}$ and in works [11,12] it was shown that the PbS films with nanoparticles from 70 to 80 nm in size have a cubic (space group $Fm\bar{3}m$) $D0_3$-type structure. In these nanofilms, PbS has the chemical formula $PbS_y^{4(b)}S_{\frac{1-y}{2}}^{8(c)}{}_y$, where $y<1$, and the sulfur atoms occupy statistically with probabilities y and $(1-y)/2$ octahedral 4(*b*) and tetrahedral 8(*c*) sites, respectively. Studies of the thermal stability of the PbS nanofilms in air [11] showed that the $D0_3$ structure remains stable at least up to a temperature of 430 K. According to [13], oxidation of the PbS nanofilms starts at a temperature above 623 K. There is no information on the thermal expansion of the PbS films in the literature though such data would be useful for applications since substrates with similar thermal expansion coefficients could be chosen for film deposition. It is very important that in situ investigation of a lattice constant of the PbS nanofilms at various temperatures allows to study thermal expansion of a crystal lattice which depends on the size of coherent scattering regions and on the change of crystal structure. The data received will also be very useful for exploration of nanofilms at elevated temperatures.

In this paper we report on an in situ study of the effect of temperature and annealing time on the structural properties of the PbS nanofilms.

2. Experimental details

Chemical bath deposition was used for the synthesis of the PbS nanofilms based on a reaction of lead acetate ($Pb(OAc)_2$) and thiourea ($(NH_2)_2CS$) in aqueous solution containing alkali and sodium citrate ($Na_3C_6H_5O_7$). As a result of hydrolysis of $(NH_2)_2CS$, sulfide ions appear in the solution and the formation and deposition of PbS sets in [14]. All nanofilms were deposited on glass substrates. The deposition was in a liquid thermostat at pH = 12 controlled by an ionometer pH/Ion Meter CyberScan 2100 (Eutech Instruments) and at $T = 325$ K. The initial concentrations of the reactants were $[Pb(AcO)_2] = 5$ mM and $[(NH_2)_2CS] = [Na_3Cit] = 25$ mM. The duration of the synthesis was 60 min. According to microinterferometric measurements the synthesized PbS films were about 100 nm in thickness.

The microstructure of the deposited film and the PbS grain size were examined by scanning electron microscopy (JEOL-JSM LA 6390). The elemental composition of the PbS films on a glass substrate was estimated

* Corresponding author at: Institute of Solid State Chemistry, The Ural Branch of the Russian Academy of Sciences, Pervomaiskaya 91, Ekaterinburg 620990, Russia. Tel.: +7 343 362 30 34.
E-mail address: sadovnikov@ihim.uran.ru (N.S. Kozhevnikova).

0040-6090/$ – see front matter © 2013 Elsevier B.V. All rights reserved.
http://dx.doi.org/10.1016/j.tsf.2013.09.079

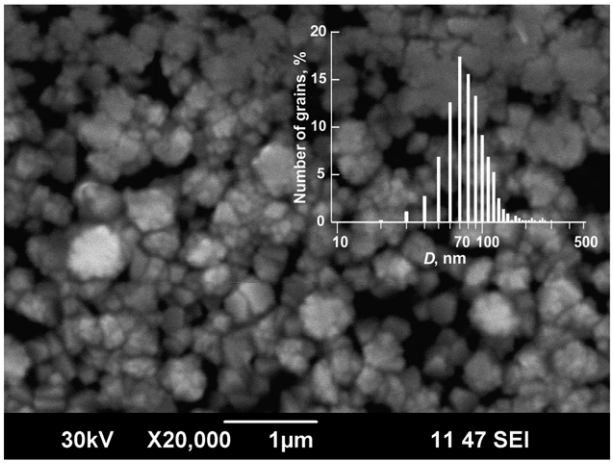

Fig. 1. Microstructure of the PbS film: PbS nanoparticles of size 60 to 100 nm are united in the agglomerates having the size up to 250 nm; the film coverage is about 80–85%. The inset shows size distributions of PbS nanoparticles in the lead sulfide nanofilms, about 50% particles are from 60 to 80 nm in size.

by the energy-dispersive X-ray (EDX) analysis (JED 2300), and the phase composition was determined by X-ray diffraction (XRD) phase analysis.

SEM images were made at multiplication from 2000 to 50,000 times, at accelerating voltage from 7 to 30 kV, and working distance of 10 mm. EDX analysis was performed using multiplication of 2000 times, accelerating voltage of 30 kV, and spot size of 44.

XRD diffraction measurements were performed in situ on a Philips X'Pert diffractometer in Bragg–Brentano geometry with Cu$K\alpha_{1,2}$ radiation in the 2θ angle interval from 18 to 90° with a step of $\Delta(2\theta) = 0.016°$, and the exposure time was 600 s for each data point. The diffractometer was equipped with a position-sensitive high-speed sector detector X'Celerator [15], which records intensity in a 2θ range of 7.2°. XRD data were taken during heating and annealing in the temperature range from 293 to 443 K.

For the annealing of the films, a ceramic furnace was heated by a stabilized current source Stab-Doppel-Labor-Netzgerät EA-3023. The temperature of the films was measured by a noncontact method with an infrared thermometer IR-1000L (Voltcraft). The uncertainty and stability was ±3 K. The substrate with the PbS nanofilm was placed directly on the heating element.

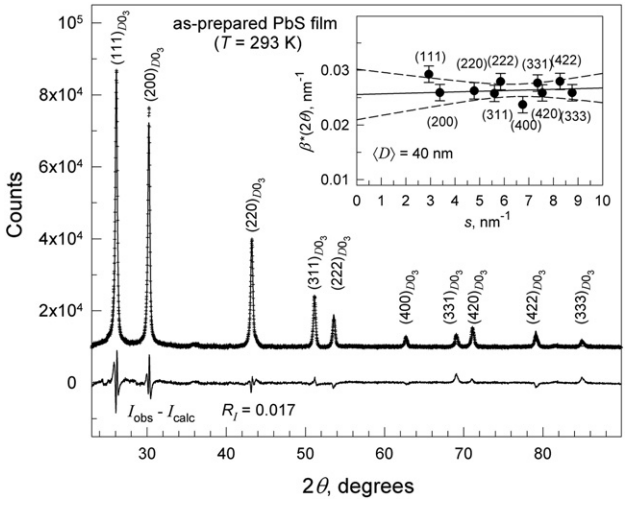

Fig. 2. Experimental (crosses) and fitted (solid line) XRD spectra with a difference plot shown in the lower part. The inset shows the reduced broadening $\beta^*(2\theta)$ where the dashed line represents the 95% confidence interval.

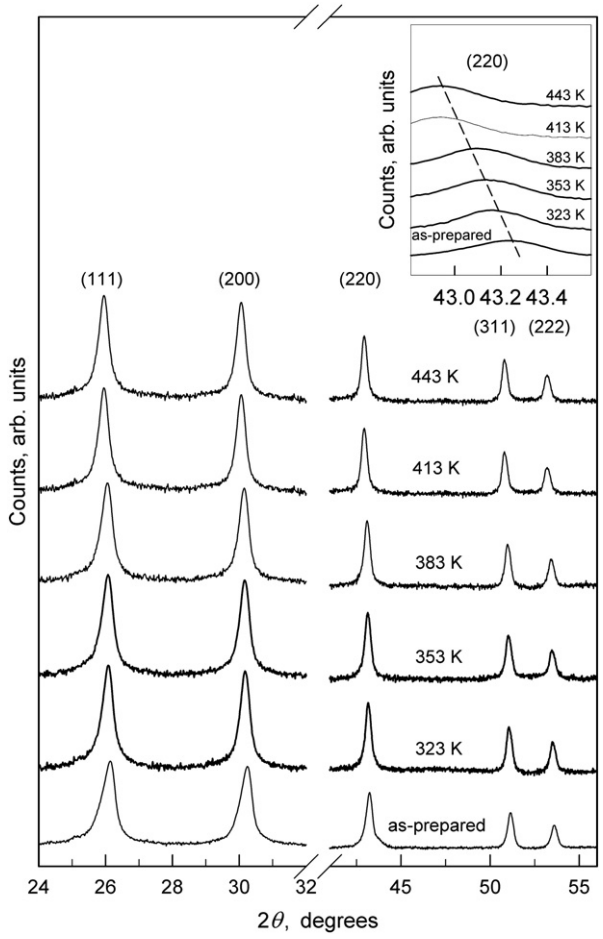

Fig. 3. XRD patterns of the PbS nanofilm during heating from 293 to 443 K. The number of counts is shown in the logarithmic scale. The inset shows the shift of the 220 reflection with increasing temperature.

The PbS nanofilm was divided before the measurements into two parts. One part was heated from 293 to 473 K in steps of 30 K. Subsequently the film was cooled to room temperature with the same steps. When the assigned temperature was reached, an XRD was taken for 6 h. The duration of measurements was 48 h for heating and for cooling. Considering that heating and cooling were slow, it can be assumed that the values of the lattice constant and of the thermal expansion coefficient were in equilibrium.

The second part of the PbS film was heated from 293 to 423 K during 1 h, and XRD patterns were taken at the 423 K after 1, 13, 19, 25, and 38 h. After 44 h the sample was cooled to 293 K and a further data set was taken.

The phase composition of the film was evaluated by the Match! © Crystal Impact program package [16], and the X'Pert Plus software suite [17] was used to determine the crystal lattice constant and for the structural refinement.

3. Results and discussion

The electron microscopy studies show nanoparticles smaller than 120 nm (Fig. 1). These nanoparticles form agglomerates with an average size of about 250 nm. Inspection of scanning electron microscopy (SEM) image reveals that the film covers not more than ~80–85% of the substrate surface. The size distributions of nanoparticles in the PbS film under study is shown in the inset. The size distribution is derived from the SEM data and is unimodal. The peak of the size distribution corresponds to particles, whose size is ~70 nm, with about one half of all particles having size in the range from 60 to 80 nm (see the inset to Fig. 1).

Because of the small thickness and the incomplete coverage of the film, the EDX analysis revealed X-ray emission lines of the chemical elements of the film (Pb, S) and of elements of the glass substrate (Si, Mg, Ca, Na, Al, O). Taking this into account the elemental composition of the film corresponds to a stoichiometric relation of Pb:S = 1:1 with an accuracy of about 1 at.%.

The XRD of the as-prepared PbS nanofilm measured at ambient temperature is shown in Fig. 2. Full profile refinement shows that the position and intensity of reflections correspond to cubic PbS with the $D0_3$ structure, in agreement with [11,12]. The lattice constant for the PbS film is 593.35 ± 0.05 pm. All observed reflections show appreciable broadening $\beta(2\theta)$ (Fig. 2). From this the average size D of coherent scattering regions and the value of microstrains ε have been estimated using the Williamson–Hall method [18,19]. The dependence of the reduced broadening $\beta^*(2\theta) = [\beta(2\theta)\cos\theta] / \lambda$ on the scattering vector $s = 2(\sin\theta) / \lambda$ for the as-prepared PbS nanofilm is shown in the inset in Fig. 2. The average size of coherent scattering regions was determined as $D = 1 / [\beta^*(2\theta)]_{s=0}$ by extrapolating $\beta^*(s)$ dependence to the zero value of s, and the microstrain ε was obtained from the slope angle φ with $\varepsilon = (\tan\varphi)/2$. Our evaluation shows that D in the as-prepared film is ~40 nm and microstrain is lacking.

The XRD patterns of the PbS nanofilm recorded in situ during heating from 293 to 443 K are presented in Fig. 3. Fig. 4 shows the XRD patterns of the PbS nanofilm recorded in situ at 423 K versus annealing time. All XRD reflections in Figs. 3 and 4 correspond to cubic PbS. The Rietveld factor R_I for all the XRD patterns does not exceed 0.018.

As seen from the inset in Fig. 3, the increase in the annealing temperature is accompanied by a systematic shift of reflections to smaller 2θ angles, which corresponds to an increase of the lattice constant. Similarly, the increase in the annealing time at 423 K is also accompanied by a shift of reflections to smaller 2θ angles (inset in Fig. 4).

Fig. 5 shows the variations of the lattice constant of the PbS nanofilm with annealing temperature from 293 to 473 K (panel *a*) and annealing time at 423 K (panel *b*). As the temperature rises from 293 to 473 K, the lattice constant increases from 593.35 to 597.50 pm. When the film is cooled to 293 K, the lattice constant decreased to 593.35 pm which coincides with the lattice constant of the as-prepared nanofilm (Fig. 5*a*). Temperature dependence of the lattice constant a (see Fig. 5*a*) is not linear and is described by quadratic function $a_T = 0.5868 + 2.164\times10^{-5}T + 2.305\times10^{-9}T^2$. During the heating of the second part of the PbS nanofilm for 1 h from ambient temperature to 423 K the lattice constant is increased from 593.35 to 595.85 pm (see Fig. 5*b*), i.e. to a value smaller than the one observed during the slow and continuous temperature rise. When the annealing time at 423 K was increased to 38 h, the lattice constant gradually grew to its maximal value of 596.37 ± 0.05 pm, which corresponds to the equilibrium value of the lattice constant at 423 K (Fig. 5*a*). This is confirmed by reaching saturation shown in Fig. 5*b*.

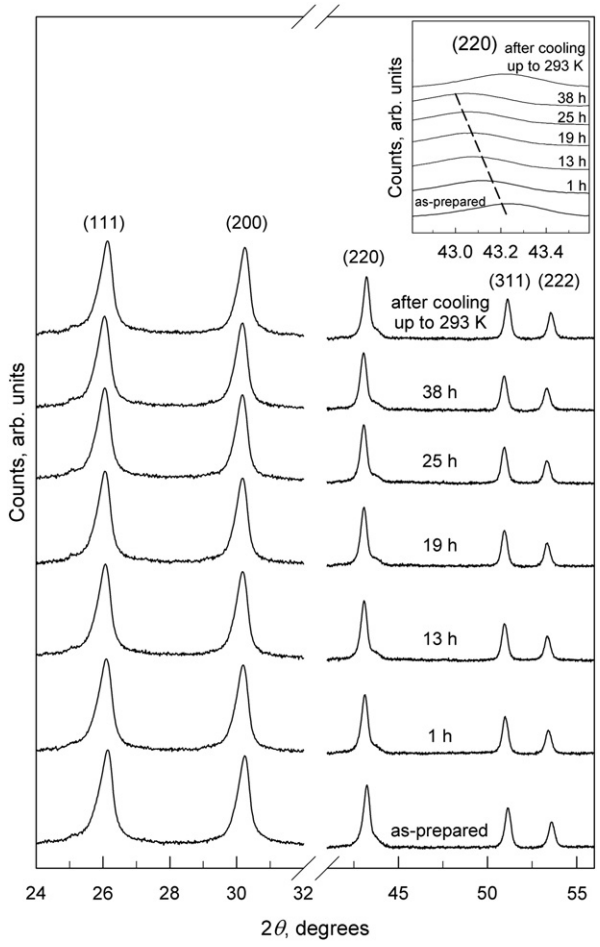

Fig. 4. XRD patterns of the PbS nanofilm obtained in situ for different annealing times at 423 K and upon cooling of the film to 293 K. The intensity is shown in logarithmic scale. The displacement of the XRD (220) reflection with an increase in the annealing duration to 38 h is shown in the inset with a dotted line.

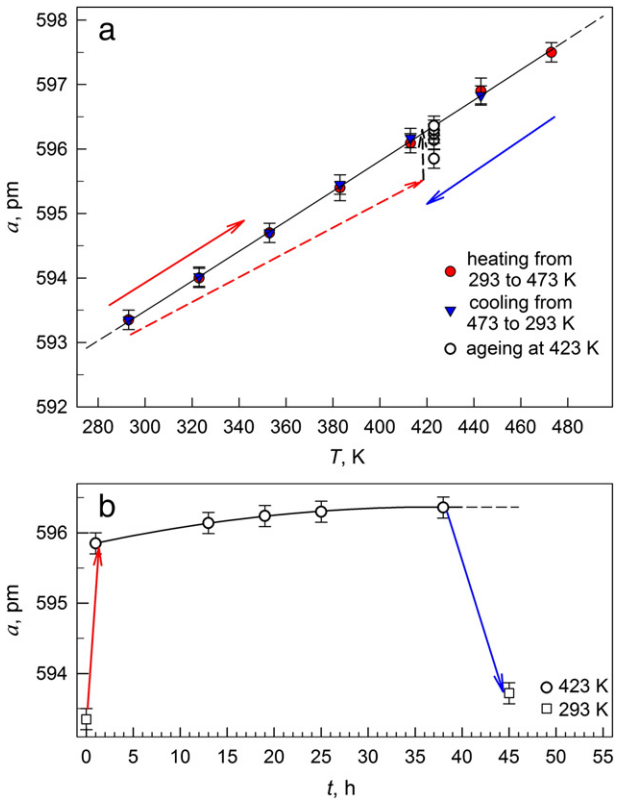

Fig. 5. Effect of temperature and annealing time on the lattice constant a_{cub} of the PbS nanofilm: (*a*) variation of the lattice constant (●) at increasing temperature from 293 to 423 K, variation of the lattice constant (▼) during cooling from 423 to 293 K, and variation of the lattice constant (**o**) during exposure of the nanofilm at a temperature of 423 K; (*b*) lattice constant a (**o**) versus duration of annealing of the nanofilm at 423 K, (□) is the lattice constant of the initial (before annealing) nanofilm measured at 293 K and measured at 293 K upon cooling of the nanofilm annealed for 38 h at 423 K. The solid and dotted arrows show the direction of the experiment during lattice constant measurement. The red dotted arrows on panel *a* and red arrow on panel *b* show the same experiment.

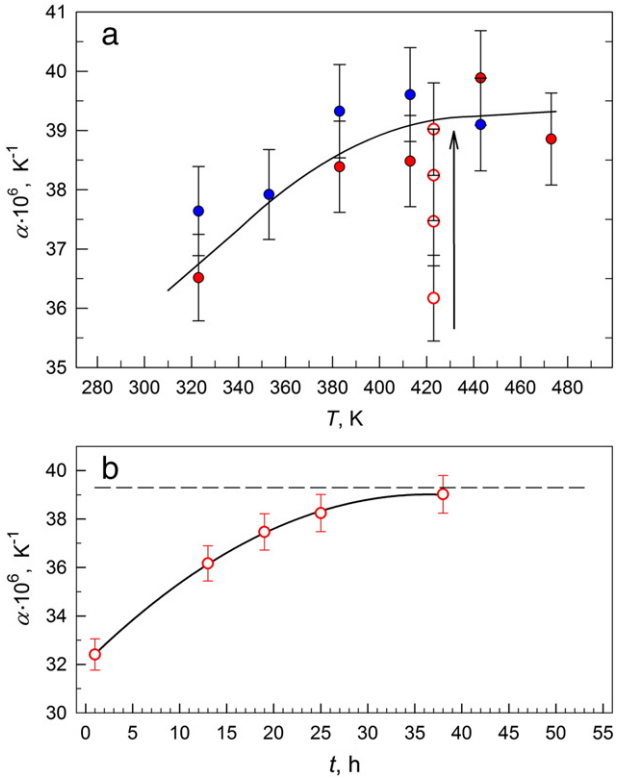

Fig. 6. Effect of temperature and annealing time on the linear thermal expansion coefficient α of the PbS nanofilm: (*a*) variation in the coefficient α (●) when the temperature increases from 293 to 423 K, (●) during cooling from 423 to 293 K, and (o) during exposure of the film at 423 K, the vertical arrow shows an increase of coefficient α at a rise of duration of annealing at a temperature of 423 K; (*b*) dependence of the coefficient α (o) on the duration of annealing of the film at 423 K.

Fig. 6 shows the temperature dependence of the thermal expansion coefficient $\alpha(T) = \frac{a_T - a_{293}}{a_{293}\,(T-293)}$, where a_T and a_{293} are the lattice constants measured at temperature T and at 293 K, respectively. The thermal expansion coefficient α increases from about 37×10^{-6} to about $39 \times 10^{-6}\,K^{-1}$ during slow heating of the PbS nanofilm from 323 to 443 K as shown in Fig. 6*a*. From Fig. 5 it is seen that heating of the film for 1 h from room temperature to 423 K does not lead to the equilibrium value of the lattice constant; that is why the thermal expansion coefficient value was small here, namely, about $32 \times 10^{-6}\,K^{-1}$. When the annealing time of the PbS nanofilm at 423 K was extended to 38 h, the coefficient α increased (Fig. 6*b*) gradually attaining saturation, i. e. it increased by the value of the thermal expansion coefficient, which is in equilibrium for the temperature of 423 K. The measurements show that relaxation processes are relevant in these nanofilms at higher temperatures. These processes are slow at the time scale of the present experiments and the equilibrium values of the lattice constant and the thermal expansion coefficient are only reached after many hours of annealing. While plotting the dependence $\alpha(T)$ (see Fig. 6*a*), annealing time was taking into consideration by an increasing determination error of thermal expansion coefficient. For example, increase in temperature on 130 K (from 293 to 423 K, see Fig. 6*b*) is accompanied by an increase of the lattice constant from 593.4 to 595.9 pm ($\Delta a = 2.5$ pm). Annealing at this temperature within 40 h leads to increase of the lattice constant only to 596.3 pm ($\Delta a = 0.4$ pm), and increase of $\Delta a = 0.2$ pm occurs at the first 10 h of annealing.

The low rate of the relaxation processes is confirmed by the small variation of the size D of coherent scattering region versus temperature and annealing time. A heating of 30 h to 413 K leads to a growth of D to 70 nm and to the appearance of a weak microstrain of 0.06%. Upon heating to 443 K, D increases to about 130 nm and the microstrain reaches 0.14% (Fig. 7). As a result of prolonged annealing of 25 h at a constant

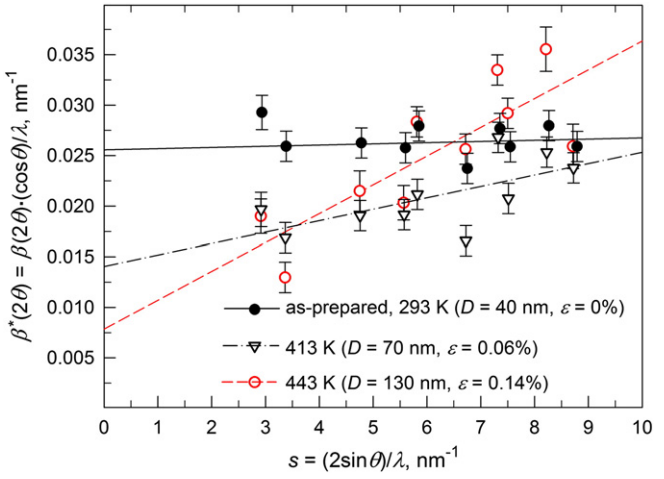

Fig. 7. Effect of the annealing temperature on the average size of the CSR and on the microstrain ε: (●) initial nanofilm at room temperature, (▽) film annealed at 413 K, and (o) film annealed at 443 K.

temperature of 423 K, a weak growth of D to about 50 ± 10 nm and a microstrain of 0.12% were observed.

The thermal expansion coefficient of the nanocrystalline PbS film can be estimated only from the data [11]. According to [11], during cooling of the PbS nanofilm from 423 to 293 K, the lattice constant decreased from 596.37 to 593.26 pm, corresponding to a thermal expansion coefficient $\alpha(423\,K) = 40 \times 10^{-6}\,K^{-1}$. When the PbS film was re-heated from 293 to 393 K, the lattice constant increased from 593.26 to 594.92 pm corresponding to a coefficient $\alpha(393\,K) = \sim 28 \times 10^{-6}\,K^{-1}$. The thermal expansion coefficient of the PbS nanofilm determined in the present work for the temperature interval from 320 to 420 K is $(37–39) \times 10^{-6}\,K^{-1}$, which is close to the value reported in [11].

The thermal expansion coefficient of polycrystalline samples of coarse-grained PbS was measured in [20,21]. In work [20], measurements were performed by interferometry at temperatures from 318 to 648 K, and in [21] the thermal expansion coefficient was measured by dilatometric method in the temperature range between 20 and 340 K yielding a thermal expansion coefficient of polycrystalline PbS at 300 K of $(19–20) \times 10^{-6}\,K^{-1}$. In [21] it was further reported that the Grüneisen constant of polycrystalline PbS monotonically decreases from 2.2 to 1.9 as the temperature rises from 20 to 340 K, and, according to [20], the Grüneisen constant increases from 1.98 to 2.26 when the

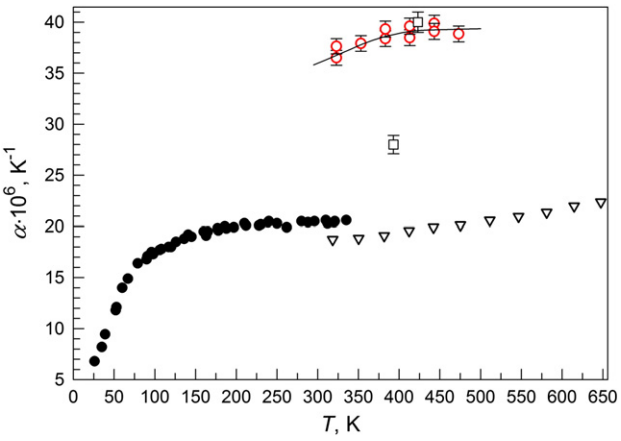

Fig. 8. Linear thermal expansion coefficient α: (●) coarse-grained polycrystalline PbS [20], (▽) coarse-grained polycrystalline PbS [21], (□) PbS film [11], and (o) results of present work for the PbS nanofilm.

temperature is raised from 320 to 670 K. Using first principles of density functional theory in quasiharmonic approximation, the authors of [22] calculated the lattice properties of PbS. According to this, the thermal expansion coefficient at 300 K is $29.8\times10^{-6}K^{-1}$ and the Grüneisen constant amounts from 2.50 to 2.52.

In Fig. 8, the results of the present work for the thermal expansion coefficient are compared with literature data [11,20,21]. It is seen that the thermal expansion coefficient of the PbS nanofilms is much larger than that for the bulk coarse-grained PbS.

The possible causes of increase in α for the PbS thin film compare to the coarse-grained PbS are the small size of the coherent scattering regions in the nanofilm and the different crystal structures, i.e. $D0_3$ type for the PbS nanofilm and $B1$ type for the coarse-grained PbS.

In present work nanosize effect on thermal expansion is observed for a binary compound. Similar effect was reported for a metal (copper Cu) [23].

4. Conclusion

As a result of the study it is found that the cubic (space group $Fm\bar{3}m$) $D0_3$–type crystal structure of the nanostructured PbS film is stable up to temperature 443 K.

The thermal expansion coefficient of the PbS nanofilm in the temperature range from 293 to 443 K is $(37–39)\times10^{-6}K^{-1}$, almost twice as large as for coarse-grained PbS. The increase in the thermal expansion coefficients α for the PbS nanofilm in comparison with that of coarse-grained PbS could be due to small size of the coherent scattering regions which leads to appearing of crystal structure $D0_3$ in the nanofilm instead of $B1$ structure in conventional thin films and leads to change of the anharmonic vibrations in nanofilm.

Acknowledgments

First author (S. S.) is grateful to A.I. Gusev for the useful discussion. This work is supported by the Russian Foundation for Basic Research (Grants Nos. 11-08-00314a and 13-08-00184a) and the Ural Division of the Russian Academy of Science (project 12-P-234-2003).

References

[1] H. Preier, Semicond. Sci. Technol. 5 (1990) S12.
[2] P.K. Nair, M.T.S. Nair, A. Fernandez, M. Ocampo, J. Phys. D. Appl. Phys. 22 (1989) 829.
[3] S. Jana, R. Thapa, R. Maity, K.K. Chattopadhyay, Phys. E. 40 (2008) 3121.
[4] S.I. Sadovnikov, N.S. Kozhevnikova, A.A. Rempel, Semiconductors 44 (2010) 1349.
[5] S.I. Sadovnikov, A.I. Gusev, J. Alloys Compd. 573 (2013) 65.
[6] H. Zogg, A. Fach, C. Maissen, J. Masek, S. Blunier, Opt. Eng. 33 (1994) 1440.
[7] A. Levchenko, L. Leonova, Yu. Dobrovolskii, Electron. Sci. Tech. Bus. 1 (2008) 66.
[8] W.W. Scanlon, J. Phys. Chem. Solids 8 (1959) 423.
[9] Y. Noda, K. Masumoto, S. Ohba, Y. Saito, K. Toriumi, Y. Iwata, K. Shibuya, Acta Crystallogr. C 43 (1987) 1443.
[10] S.B. Qadri, A. Singh, M. Yousuf, Thin Solid Films 431–432 (2003) 506.
[11] S.I. Sadovnikov, A.A. Rempel, Phys. Solid State 51 (2009) 2375.
[12] S.I. Sadovnikov, A.A. Rempel, A. Magerl, in: V.E. Borisenko, S.V. Gaponenko, V.S. Gurin (Eds.), Proceedings of the International Conference on Nanomeeting—2009, Physics, Chemistry and Application of Nanostructures, Minsk, Belarus, May 26–29, 2009, 2009, p. 341.
[13] S.I. Sadovnikov, N.S. Kozhevnikova, A.A. Rempel, Russ. J. Inorg. Chem. 56 (2011) 1864.
[14] N.S. Belova, A.A. Uritskaya, G.A. Kitayev, Russ. J. Appl. Chem. 75 (2002) 1598.
[15] R.W. Morton, D.E. Simon, J.J. Gislason, S. Taylor, Adv. X-ray Anal. 46 (2003) 80.
[16] Match! Phase identification from powder diffraction, Version 1.9a © 2003–2009 Crystal Impact, 2009. (Jan15th).
[17] X'Pert Plus Version 1.0, Program for crystallography and Rietveld analysis Philips Analytical B. V. © Koninklijke Philips Electronics N. V. 1998-1999.
[18] W.H. Hall, Proc. Phys. Soc. Lond. Sect. A 62 (1949) 741.
[19] W.H. Hall, G.K. Williamson, Proc. Phys. Soc. Lond. Sect. B 64 (1951) 937.
[20] S.S. Sharma, Proc. Indian Acad. Sci. A A34 (1951) 72.
[21] S.I. Novikova, N.K. Abrikosov, Sov. Phys. Solid State 5 (1963) 1558.
[22] Yi Zhang, X. Ke, C. Chen, J. Yang, P.R.C. Kent, Phys. Rev. B B80 (2009)(paper 024304).
[23] A.I. Gusev, A.A. Rempel, Nanocrystalline Materials, Cambridge Int. Science Publishing, Cambridge, 2004.